Acta Crystallographica Section D
Biological Crystallography
ISSN 0907-4449

Structure of staphylococcal enterotoxin C2 at various pH levels

D. Kumaran,[a,b] S. Eswaramoorthy,[a] W. Furey,[b,c] M. Sax[b] and S. Swaminathan[a]*

[a]Biology Department, Brookhaven National Laboratory, Upton, NY 11973, USA, [b]Biocrystallography Laboratory, VA Medical Center, Pittsburgh, PA 15240, USA, and [c]Department of Pharmacology, University of Pittsburgh, Pittsburgh, PA 15261, USA

Correspondence e-mail: swami@bnl.gov

Received 15 February 2001
Accepted 3 July 2001

PDB References: SEC2, tetragonal, pH 5, 1cqv; SEC2, tetragonal, pH 5.5, 1i4p; SEC2, tetragonal, pH 6, 1i4q; SEC2, tetragonal, pH 6.5, 1i4r; SEC2, monoclinic, pH 8, 1i4x.

The three-dimensional structure of staphylococcal enterotoxin C2 (SEC2), a toxin as well as a superantigen, has been determined at various pH levels from two different crystal forms, tetragonal (pH 5.0, 5.5, 6.0 and 6.5) and monoclinic (pH 8.0) at 100 and 293 K, respectively, by the molecular-replacement method. Tetragonal crystals belong to space group $P4_32_12$, with unit-cell parameters $a = b = 42.68$, $c = 289.15$ Å (at pH 5.0), and monoclinic crystals to space group $P2_1$, with unit-cell parameters $a = 43.3$, $b = 70.6$, $c = 42.2$ Å, $\beta = 90.3^\circ$. SEC2 contains a zinc-binding motif, D+HE*xx*H, and accordingly a Zn atom has been identified. The coordination of the zinc ion suggests that it may be catalytic zinc rather than structural, but there is so far no biological evidence that it possesses catalytic activity. However, superantigen staphylococcal exfoliative toxins A and B have been shown to have enzymatic activity after their fold was identified to be similar to that of serine protease. The structure and its conformation are similar to the previously reported structures of SEC2. Though it was expected that the zinc ion may be leached out, as the histidines coordinating the zinc ion are expected to be protonated below pH 6.0, zinc is present at all pH values. The coordination distances to zinc increase with decreasing pH, with the distances being the least at pH 8.0. The results of automated model building using the *ARP*/*wARP* program for different data sets collected at various pH values are discussed.

1. Introduction

Staphylococcus aureus produces six serotypes (A to F) of enterotoxins (SEs), with three antigenically distinct subtypes for type C. SEs are released as a single polypeptide chain with molecular mass in the range 22–29 kDa and share significant sequence homology (Marrack & Kappler, 1990; Ren *et al.*, 1994). The amino-acid sequence identity ranges from 25 to 83%, with SEA and SEE having the highest sequence similarity (Betley *et al.*, 1992). They all induce vomiting and diarrhea in humans (Bergdoll, 1979, 1985). They also have been identified as superantigens, as they cause proliferation of T-cell receptors (TCR) when presented by the major histocompatibility complex class II molecules (MHCII). This is attributed to the fact that in the MHCII–SE–TCR complex only the Vβ element of TCR comes into contact with the SE and there are only a limited number of Vβ elements available in humans (Kappler *et al.*, 1989; White *et al.*, 1989). Hence, a subset of TCRs bearing a particular Vβ element is activated. Unlike antigenic peptides, intact SEs bind to MHCII without being processed. Antigenic peptides are still present in the MHCII peptide-binding groove, but its ability to invoke TCR

activation is probably suppressed by the wedge formed between TCR and MHCII as suggested by a hypothetical ternary complex model (Fields *et al.*, 1996). Though all SEs have similar folds, they have different Vβ specificities with some overlap.

The presence of a zinc ion has previously been reported in the staphylococcal enterotoxin C2 (SEC2) crystal structure (Papageorgiou *et al.*, 1995), but the role of the zinc ion is not yet understood. Furthermore, it has been suggested that the zinc may not be bound to SEC at acidic pH, as the histidines coordinated to the zinc ion are supposed to be crucial residues responsible for emetic activity and these histidines are free in other SEs. To study the effect of pH on the zinc-binding site in SEC2 and its conformation, the protein was crystallized at different pH values, 5.0, 5.5, 6.0, 6.5 and 8.0, and the structures were determined.

2. Materials and methods

2.1. Crystallization

SEC2 was obtained as a gift from USAMRIID, Fort Detrick, USA. The lyophilized protein contained 0.2 *M* sodium phosphate, which was removed by dialysis against deionized water overnight. The crystals were grown as described in Swaminathan *et al.* (1995*a*) at four different pH levels (5.0, 5.5, 6.0 and 6.5) at room temperature by the sitting-drop vapor-diffusion method. 2 µl protein solution (5 mg ml^{-1}) and 2 µl precipitant solution containing 20% PEG 8000, 0.2 *M* magnesium acetate and 0.1 *M* sodium cacodylate buffer at the appropriate pH were mixed and equilibrated against 800 µl of the same precipitant solution. Crystals appeared within a few days and grew to their full size in 10 d. Interestingly, SEC2 could be crystallized over a wide range of pH values from pH 5.0 to 8.0. Crystals at pH 8.0 were crystallized with 20% PEG 6000, 0.1 *M* Tris–HCl. The crystal structure reported previously was at pH 7.0 (Swaminathan *et al.*, 1995*b*).

2.2. Data collection

Data from monoclinic crystals were collected at room temperature with a Siemens Hi-Star area detector mounted on a Rigaku RU-200 rotating-anode X-ray generator with a crystal-to-detector distance of 120 mm and $2\theta = 16^\circ$. An oscillation range of 0.25° was used and data corresponding to 180° rotation were collected and processed with *XENGEN* (Howard *et al.*, 1987). Scaling of the data was performed with a locally modified version of Weissman's scaling program (Weissman, 1982). Data from tetragonal crystals were collected at liquid-nitrogen temperature by first transferring the crystals into a cryoprotectant. The cryoprotectant was similar to the precipitant used for crystallization, except that PEG 8000 was substituted by PEG 1000. Use of lower molecular weight PEG was found to be more suitable as cryoprotectant (Garman & Mitchell, 1996). Crystals were picked up in Hampton loops and immediately flash-frozen by dipping into liquid nitrogen. The frozen crystals were mounted on a goniometer head and the data were collected at 100 K on beamline X12B of the National Synchrotron Light Source (NSLS) at Brookhaven National Laboratory, USA. Data were collected at a wavelength of 0.978 Å using an oscillation range of 1.0° and a crystal-to-detector distance of 300 mm with a Quantum 4 detector. Since it was known from the preliminary studies that one of the unit-cell parameters is about 300 Å, the following strategy was used to resolve the spots in the detector and to collect high-angle data. The crystal-to-detector distance was set at 300 mm and the 2θ arm was offset by 10°. In addition, the detector was displaced horizontally, perpendicular to the X-ray beam, to collect higher resolution data. Data were processed with *DENZO* and *SCALEPACK* (Otwinowski & Minor, 1997). The crystals belong to the tetragonal space group $P4_32_12$, with unit-cell parameters $a = b = 42.68$, $c = 289.15$ Å (at pH 5.0) and a single SEC2 molecule per asymmetric unit. The data sets of SEC2 at pH 5.0, 5.5, 6.0, 6.5 and 8.0 are subsequently referred to as SE50, SE55, SE60, SE65 and SE80, respectively. Details of the crystal parameters and data-collection statistics are presented in Table 1.

2.3. Structure solution and refinement

The structures of the tetragonal crystals were solved by the molecular-replacement method with the program *AMoRe* (Navaza & Saludjian, 1997), with the coordinates from monoclinic crystal form (PDB code 1se2) as a search model (Swaminathan *et al.*, 1995*a*). The details for SE50 alone are given here. The rotational and translational search using data to 3.5 Å gave a single solution, which gave an *R* factor of 38.2% and correlation coefficient 64.9% after rigid-body refinement in *AMoRe*. The calculations were repeated for the enantiomorphic space groups $P4_12_12$ and $P4_32_12$. The final statistics were far superior for the space group $P4_32_12$ and confirmed the original choice of the space group. Phases from the initial model were subjected to solvent flattening with the program *PHASES* (Furey & Swaminathan, 1997) and were used in the *ARP*/*wARP* (Perrakis *et al.*, 1999) procedure to build the model automatically. The *ARP*/*wARP* program combines an iterative manner reciprocal-space structure-factor refinement and updating of the model in real space. For SE50, *ARP*/*wARP* gave eight chains containing 181 residues of the possible 239, with 42.5% of side chains automatically placed. The rest of the model was built manually with *O* (Jones *et al.*, 1991). Details of the *ARP*/*wARP* procedure for all five structures are given in Table 1.

Further refinement was carried out with *REFMAC* (Murshudov *et al.*, 1997). 5% of the reflections were used for the calculation of $R_{\rm free}$ (Brünger, 1992). 15 179 reflections in the resolution range 12.5–2.06 Å were used throughout the refinement. After 12 cycles of refinement, the *R* factor and $R_{\rm free}$ converged to 27 and 31.2%, respectively. The $F_o - F_c$ map showed a strong peak (12σ) corresponding to the zinc ion. Even though the data were collected at 0.98 Å and not at the zinc absorption edge (1.2837 Å), an anomalous difference Fourier phased with the phases generated with the model

Table 1
Data collection, processing, *ARP/wARP* and refinement statistics of SEC2.

Name/code	SE50†	SE55‡	SE60‡	SE65‡	SE80§
PDB code	1cqv	1i4p	1i4q	1i4r	1i4x
Unit-cell parameters					
a (Å)	42.68	43.16	42.68	42.73	43.3
b (Å)	42.68	43.16	42.68	42.73	70.6
c (Å)	289.15	291.28	288.37	288.54	42.2
β (°)	—	—	—	—	90.3
Space group	$P4_32_12$	$P4_32_12$	$P4_32_12$	$P4_32_12$	$P2_1$
Resolution range (Å)	42.23–2.06	39.44–1.99	42.22–2.20	42.27–2.07	38.0–2.3
Total No. of reflections	82018	67434	73277	66686	24947
No. of unique reflections	16097	15905	13934	14722	9146
Redundancy	5.1	4.2	5.2	4.5	2.8
No. rejected	150	83	125	150	658
Mosaicity	0.284	0.414	0.243	0.347	—
Completeness (overall) (%)	91.1	78.5	95.1	83.4	80.6
Completeness (last shell) (%)	48.0	30.5	56.7	29.7	16.2
$R_{\rm merge}$ (F^2)¶ (overall)	3.0 (5.0)	4.4 (6.0)	2.4 (6.0)	3.3 (6.5)	8.6
$\langle I/\sigma(I)\rangle$	33.6	25.7	30.6	27.4	—
ARP/wARP results					
Total No. of residues	239	239	239	239	—
No. of chains	8	17	16	12	—
No. of residues modeled automatically	181	111	117	146	—
No. of side chains modeled automatically (%)	42.5	10.8	19.7	15.1	—
Refinement statistics					
Resolution (Å)	12.5–2.06	50.0–2.0	50.0–2.2	50.0–2.1	10.0–2.4
R factor††/$R_{\rm free}$ (%)	20.8/28.0	20.6/26.3	21.3/25.4	20.2/24.4	20.7
R.m.s deviations from ideality					
Bond lengths (Å)	0.187	0.010	0.010	0.010	0.012
Bond angles (°)	3.3	1.57	1.30	1.30	2.34
Average *B* factors (Å^2)					
Main chain	22.6	16.6	12.6	12.3	8.26
Side chain	23.6	17.9	14.4	14.3	11.21
Solvent	29.5	24.9	22.0	23.0	18.45
No. of protein atoms	1865	1907	1907	1907	1915
No. of solvent molecules	163	224	176	229	91
No. of metal atoms	1	1	1	1	1
Residues (%) in the core region of φ–ψ plot	86.3	87.8	85.0	86.4	81.8

† Refined with *REFMAC*. ‡ Refined with *CNS*. § X-ray data collected with Siemens Hi-Star area detector and refined with *X-PLOR* 3.1. ¶ $R_{\rm merge} = \sum_j |I_h - \langle I\rangle_h|/\sum I_h$, where $\langle I\rangle_h$ is the average intensity over symmetry equivalents; the values given in the parentheses are for the outermost shell. †† *R* factor = $\sum |F_{\rm obs} - F_{\rm calc}|/\sum |F_{\rm obs}|$.

before including zinc showed a peak of 20σ at the zinc position, also confirming the presence of zinc (Fig. 1). The *R* factor fell to 26.2% ($R_{\rm free}$ = 30.3%) with the zinc ion included in the refinement. A total of 163 water molecules were automatically placed and refined using *REFMAC* cycled with *ARPP* (Lamzin & Wilson, 1993). The water molecules were also checked in the $2|F_o| - |F_c|$ map for consistency. A similar procedure was followed for SE55, SE60 and SE65. However, the program *CNS* (Brunger *et al.*, 1998) was used for refinement with these data sets (Table 1).

For the monoclinic crystal form, coordinates from 1se2 were used for initial rigid-body refinement. Further refinements were carried out with *X-PLOR* 3.1.

3. Quality of the model

The final refined model of SEC2 at pH 5.0 contains 1865 non-H atoms (232 residues), one Zn^{2+} ion and 163 water molecules. The quality of the protein model was good as assessed by the program *PROCHECK* (Laskowski *et al.*, 1993). All the backbone torsion angles (Φ, Ψ) lie within the allowed regions of the Ramachandran plot (Ramakrishnan & Ramachandran, 1965). Residues Asp99–Thr105 in the disulfide loop are disordered and no electron density was observed. The disulfide loops in all the SEs are highly susceptible to proteolysis and are disordered in the crystal structures reported so far.

4. Results and discussion

4.1. Structure description

The of SEC2 molecule consists of two domains (Fig. 2) which are linked together by a loop. Three helices and a β-barrel containing five β-strands (β1–β5) constitute the N-terminal domain (residues 1–120). The core of the β-barrel region is hydrophobic and it is capped by the α-helix α3 at one end. This domain has been described as an oligosaccharide/oligonucleotide binding (OB) fold (Murzin, 1993). The C-terminal domain (residues 127–239) resembles the β-grasp motif in immunoglobulin-binding domains, ubiquitin, 2Fe–2S ferrodoxin and translation initiation factor 3, as noted by the SCOP database (Murzin *et al.*, 1995). This domain contains a long helix (α3) and twisted β-sheet (β6–β12) structure. It also contains the helix α4 which is partly a 3_{10} helix. The interactions between the α-helices (α3 and α4) pack the two domains tightly.

4.2. Comparison with the earlier structures

The overall fold of the refined SEC2 structure at various pH levels is identical to the structures determined at pH 7.0 (Swaminathan *et al.*, 1995*b*) and 6.5 (Papageorgiou *et al.*, 1995). The backbone atoms superpose well, with an r.m.s. deviation of less than 1 Å (Fig. 3). There is no significant difference in the structures except in the two loop regions (residues 54–59 and residues 118–123), which take slightly different conformations. The side-chain conformations of residues in the loop region 54–59 are also different. Region 118–123 is the zinc-binding region, which might explain the difference in the conformation, as the zinc–ligand distances vary with pH. The differences are probably a consequence of

Figure 1
Stereoviews of electron density corresponding to zinc in $F_o - F_c$ and anomalous difference Fourier maps are shown in blue (5σ) and red (10σ) for the structure determined at pH 5.0. The refined zinc position is superposed on the residual density. Coordinating protein atoms are shown in ball-and-stick representation.

Figure 2
A *RIBBONS* (Carson, 1991) representation of SEC2. The zinc ion and coordination ligands are shown in ball-and-stick representation. α-Helices and 3_{10} helices are shown in red and blue, respectively.

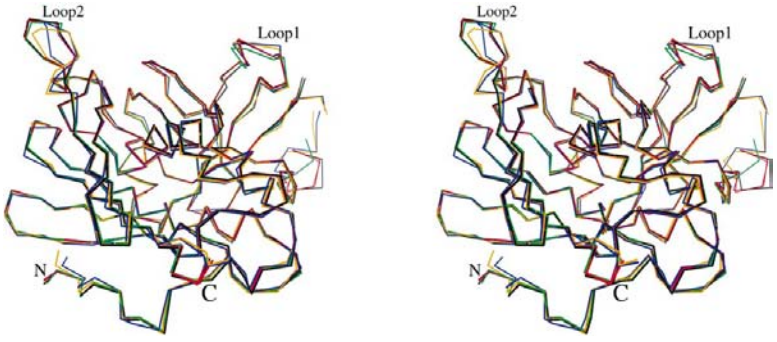

Figure 3
Stereoview of C^{α} superposition of SEC2 determined at pH 5.0 (green), 5.5 (black), 6.0 (red), 6.5 (maroon), 7.0 (blue) and 8.0 (orange). The structure at pH 7.0 was reported earlier (Swaminathan *et al.*, 1995*b*). There is no significant difference in the structures except in the two loop regions (residues 54–59 and residues 118–123, marked as loop1 and loop2), which take slightly different conformations. The differences in the disulfide-loop region (93–110) are a consequence of disorder. The breaks in the disulfide loop arise from missing residues.

the mobility of these regions. The average thermal factors for atoms in these loops are much greater than the average thermal factor for the whole molecule. The differences in the disulfide-loop region (93–110) are probably a consequence of the disorder present in that region. Maximum differences in side-chain conformations occur for charged residues which are either on the surface of the molecule or exposed to the solvent.

4.3. Disulfide loop and zinc-binding site

In all staphylococcal enterotoxins a disulfide bridge is present and it has been suggested that this loop may be responsible for the emetic properties of staphylococcal enterotoxins (Hovde *et al.*, 1994). In SEC2, there are 16 residues in between the contributing cysteine residues (Cys93–Cys110). This loop is highly flexible and residues 93–108 are disordered.

In SEA and SEE, a zinc ion is present and is bound to the C-terminal domain of the toxin and is reportedly required for SE to bind to MHCII (Fraser & Hudson, 1993; Fraser *et al.*, 1992; Sundstrom *et al.*, 1996). In SEC2 (and, by extension, in all SECs) a zinc ion is found to be bound close to the N-terminal domain, although its structural or functional role is not yet clear. Papageorgiou *et al.* (1995) proposed that zinc may not be bound to SEC when present in the gut at acidic pH. However, in the present structure of SEC2 at pH 5.0, the presence of zinc is confirmed both from $F_o - F_c$ and anomalous difference Fourier maps. The zinc ion is tetrahedrally coordinated to Asp83, His118, His122 and to Asp9 of a translation-related molecule (Fig. 4). In the monoclinic crystal form (pH 8.0), the zinc ion is located between two molecules related by a similar translation. However, the side chain of Asp9 of the translated molecule takes a different orientation and does not coordinate to the zinc ion. The electron-density maps do not support the fourth coordination both at pH 7.0 (Swaminathan *et al.*, 1995*b*) and pH 8.0. The distance between Asp9 OD2 and zinc is greater than 6 Å and disorder or a high thermal factor cannot explain the absence of this coordination. A large rotation of χ_1 and χ_2 (112 and 107°) will be required to bring this atom to a coordinating distance. Hence, this may be an artifact of packing and the lattice forces. His188 is conserved in all SEs except toxic shock syndrome toxin and has been implicated in emetic activity. Carboxymethylation of all histidines in SEA completely abrogated all the biological activities of SEA, suggesting that histidines play a role in the biological function. Though His118 is a conserved residue, in SECs it takes part in zinc coordination and it has accordingly been suggested that it may not be responsible for emetic activity. At the acidic pH 5.0, since histidines may be protonated, the His118 may be free and may still be responsible for emetic activity. However, in this structure, where the crystallization was performed at pH 5.0, zinc is still present and coordinated to the protein atoms, though with a reasonable difference

Table 2
Coordination geometry of zinc ion in SEC2 at different pH values.

	SE50	SE55	SE60	SE65	SE70†‡	SE80‡
Coordination distance (Å)						
Zn—OD2 Asp83	2.17	2.07	2.08	1.95	1.94	1.90
Zn—ND1 His118	2.34	2.29	2.21	2.20	2.05	1.96
Zn—NE2 His122	2.23	2.22	2.17	2.19	2.04	1.95
Zn—OD2 Asp9§	2.21	2.03	2.07	2.08	—	—

† Previously reported work. ‡ Coordination to symmetry-related molecule is absent. § Symmetry-related molecule.

Table 3
Thermal factors (Å^2) for zinc and its ligands.

	SE50	SE55	SE60	SE65	SE80
Zn240	19.89	12.28	10.51	10.29	10.66
His118 ND1	19.74	13.83	11.02	11.12	7.86
His122 NE1	22.95	14.68	13.05	12.55	5.56
Asp9 OD2	21.04	14.19	9.49	10.87	24.39

in the geometry of coordination. The coordination distances for zinc at various pH values are given in Table 2. Thermal factors for zinc and its ligands are given in Table 3. In general, the coordination distances decrease with increasing pH within experimental error. The coordination distances for zinc at pH 5.0 are much larger than at pH 8.0 (Fig. 4). This suggests that the coordination geometry of the zinc has been distorted from the normal values. At very high acidic pH, the zinc may be removed completely, although at present there is no crystallographic evidence for this.

The presence of zinc in a macromolecule has been classified as structural or catalytic depending on the zinc-coordination motif (Vallee & Auld, 1990*a*,*b*). In general, catalytic zinc will have three coordinations to protein atoms and one to an activated water molecule, whereas structural Zn atoms will be coordinated by four protein ligands. The zinc coordination in SEC suggests that it may be catalytic zinc rather than structural zinc, where a nucleophilic water molecule might have been replaced by a symmetry-related protein atom in the crystal structure because of crystal packing. The zinc site and its coordination in SEC2 are very similar to those in thermolysin and *Clostridium botulinum* neurotoxins (Lacy *et al.*, 1998; Swaminathan & Eswaramoorthy, 2000), which are zinc endopeptidases. However, in both of these the zinc-binding motif is HE*xx*H+E, where the second glutamate residue is separated by 34 or 36 residues from the second histidine. In SEC2 the zinc motif is D+HE*xx*H and the aspartate residue is separated by 35 residues from the first histidine. The fold and the secondary structures involved in zinc binding are different in all three proteins. Superposition of zinc-coordination residues in SEC2 and the recently solved BoNT/B structure gives an r.m.s. deviation of 1.9 Å for the main-chain atoms. The nucleophilic water corresponds to the OD2 of the symmetry-related Asp9 in SEC2, suggesting that in solution this coordination may be replaced with a water. However, the biological function of this zinc, if not catalytic, is still not clear. In SEA and SEE it has been suggested this zinc might form a bridge between His81 of the α domain of MHCII, but the hypothetical model of the ternary complex of MHCII–SEC2–TCR Vα, Vβ places this zinc away from any of the interfaces between the proteins (Fields *et al.*, 1996). It is possible that not all SEs bind similarly to MHCII. The mode of binding of SEB and TSST1 to MHCII has already been shown to be different (Jardetzky *et al.*, 1994; Kim *et al.*, 1994). Studies with deletion mutation in SEC1 and with peptides corresponding to 74—86, 148–162 and 156–171 of SEC1 may suggest that the mode of binding of SEC1 to MHCII may be different and may involve the groove created by α4, in which case the Zn atom may be close to the MHCII molecule (Hoffmann *et al.*, 1994). However, with the available experimental evidence, we tend to conclude that this zinc may be structural only. However, staphylococcal exfoliative toxins A and B, which are also superantigens, have been identified recently as serine proteases (Vath *et al.*, 1997, 1999) after their fold was discovered by crystal structure analysis.

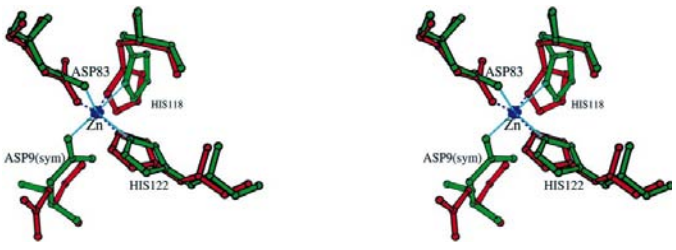

Figure 4
Stereoview in ball-and-stick representation of zinc and coordinating ligands. Coordinating geometry at pH 5.0 (green) and 8.0 (red) are shown. Zinc coordinations are represented by thin and dashed lines for SE50 and SE80, respectively. Coordination from the symmetry-related Asp9 is not present at pH 8.0 as the side chain takes a different conformation. Figs. 1, 3 and 4 were created using *MOLSCRIPT* (Kraulis, 1991).

4.4. *ARP*/*wARP* results

The availability of four data sets collected from similar crystals allowed us to draw some limited conclusions regarding the success of *ARP*/*wARP*. The high-resolution data for these crystals ranged from 1.99 to 2.2 Å (Table 1). Though SE55 has the highest resolution data, the completeness is only 78.5%, whereas SE60 has the lowest value for high resolution and its completeness is 95.1%. As can be seen, *ARP*/*wARP* gave only 111 and 117 residues of a possible 239 residues. For SE55, the completeness in the highest resolution shell was also 30.5%, compared with 56.7% for SE60. The resolution limits for SE50 and SE65 were almost the same, but the completeness was 91.1% for SE50, higher than the 83.4% for SE65. Accordingly, the numbers of residues obtained from *ARP*/*wARP* were 181 and 146 for SE50 and SE65, respectively. Additionally, the completenesses in the highest shell are 48 and 29.7%, respectively. Therefore, considering the resolution limit and the completeness, it appears that for *ARP*/*wARP* to work best, not only higher resolution (preferably to 2.0 Å) data are required, but also the overall completeness and the comple-

teness in the highest shell play a role in its success. In addition, a low $R_{\rm merge}$ value also plays a role. However, for SE60, which has the lowest $R_{\rm merge}$ value in spite of high redundancy, the method was less successful than for SE50, which had similar redundancy but a slightly higher $R_{\rm merge}$. Our experiments suggest that high-resolution data with maximum completeness and good $R_{\rm merge}$ with high redundancy are required for *ARP*/*wARP* to be successful. It is also seen that the percentage of the number of side chains placed correctly is highest for SE50, which is the best data set of the four sets presented here. We believe that, although this analysis is very limited, this information will be useful in structural genomics projects where high-throughput model building with minimum manual intervention is desired. However, these trials were carried out with *ARP*/*wARP* version 5.0. The algorithm has been improved further and the resolution limit need not now be as high as 2.0 Å. Although these structures were solved with the molecular-replacement method for model building, we used the option of using the phases rather than the coordinates. Such a procedure was also successfully used for the *C. botulinum* type B structure (Swaminathan & Eswaramoorthy, 2000).

We would like to thank James Hartling, Aravind Swaminathan and Hayley Salomon for their help in model building. Research supported by the Chemical and Biological Nonproliferation Program NN20 of the US Department of Energy under Prime Contract No. DE-AC02-98CH10886 with Brookhaven National Laboratory and the US Department of Veterans Affairs.

References

Bergdoll, M. S. (1979). *Food-borne Infections and Intoxications*, edited by H. Reimann & F. L. Bryan, pp. 443–494. New York: Academic Press.

Bergdoll, M. S. (1985). In *The Staphylococci*, edited by J. Jeljaszwicz. New York: Gustav Fisher Verlag.

Betley, M. J., Borst, D. W. & Regassa, L. B. (1992). *Chem. Immunol.* **55**, 1–35.

Brünger, A. (1992). *Nature (London)*, **355**, 472–475.

Brunger, A. T., Adams, P. D., Clore, G. M, Delano, W. L., Gros, P., Grosse-Kunstlere, R. W., Jiang, J.-S., Kuszewski, J., Nilges, N., Pannu, N. S., Read, R. J., Rice, L. M., Simonson, T. & Warren, G. L. (1998). *Acta Cryst.* D**54**, 905–921.

Carson, M. (1991). *J. Appl. Cryst.* **24**, 958–961.

Fields, B. A., Malchiodi, E. L., Li, H., Ysern, X., Stauffacher, C. V., Schlievert, P. M., Karjalainen, K. & Mariuzza, R. A. (1996). *Nature (London)*, **384**, 188–192.

Fraser, J. D. & Hudson, K. R. (1993). *Res. Immunol.* **144**, 188–193.

Fraser, J. D., Urban, R. G., Strominger, J. L. & Robinson, H. (1992). *Proc. Natl Acad. Sci. USA*, **89**, 5507–5511.

Furey, W. & Swaminathan, S. (1997). *Methods Enzymol.* **276**, 590–620.

Garman, E. F. & Mitchell, E. P. (1996). *J. Appl. Cryst.* **29**, 584–587.

Hoffmann, M. L., Jablonski, L. M., Crum, K. E., Hackett, S. P., Chi, Y.-I., Stauffacher, C. V., Stevens, D. L. & Bohach, G. A. (1994). *Infect. Immun.* **62**, 3396–3407.

Hovde, C. J., Marr, J. C., Hoffmann, M. L., Hackett, S. P., Chi, Y. I., Crum, K. K., Stevens, D. L., Stauffacher, C. V. & Bohach, G. A. (1994). *Mol. Microbiol.* **13**, 897–909.

Howard, A. J., Gilliland, G. L., Finzel, B. C. & Poulos, T. L. (1987). *J. Appl. Cryst.* **20**, 383–387.

Jardetzky, T. S., Brown, J. H., Gorga, J. C., Stern, L. J., Urban, R. G., Chi, Y.-I., Stauffacher, C. S., Strominger, J. L. & Wiley, D. C. (1994). *Nature (London)*, **368**, 711–718.

Jones, T. A., Zou, J., Cowan, S. & Kjeldgaard, M. (1991). *Acta Cryst.* A**47**, 110–119.

Kappler, J., Kotzin, B., Herron, L., Gelfand, E. W., Bigler, R. D., Boylston, A., Carrel, S., Posneit, C. D., Choi, Y. & Marrack, P. (1989). *Science*, **244**, 811–814.

Kim, J. S., Urban, R. G., Strominger, J. L. & Wiley, D. C. (1994). *Science*, **266**, 1870–1874.

Kraulis, P. J. (1991). *J. Appl. Cryst.* **24**, 946–950.

Lacy, D. B., Tepp, W., Cohen, A. C., DasGupta, B. R. & Stevens, R. C. (1998). *Nature Struct. Biol.* **5**, 898–902.

Lamzin, V. & Wilson, K. S. (1993). *Acta Cryst.* D**49**, 129–147.

Laskowski, R. A., MacArthur, M. W., Moss, D. S. & Thornton, J. M. (1993). *J. Appl. Cryst.* **26**, 283–291.

Marrack, P. & Kappler, J. (1990). *Science*, **248**, 705–711.

Murshudov, G. N., Vagin, A. A. & Dodson, E. J. (1997). *Acta Cryst.* D**53**, 240–255.

Murzin, A. G. (1993). *EMBO J.* **16**, 861–867.

Murzin, A. G., Brenner, S. E., Hubbard, T. & Chothia, C. (1995). *J. Mol. Biol.* **247**, 536–540.

Navaza, J. & Saludjian, P. (1997). *Methods Enzymol.* **276**, 581–594.

Otwinowski, Z. & Minor, W. (1997). *Methods Enzymol.* **276**, 307–326.

Papageorgiou, A. C., Acharya, K. R., Shapiro, R., Passalacqua, E. F., Brehm, R. L. & Tranter, H. S. (1995). *Structure*, **3**, 769–779.

Perrakis, A., Morris, R. & Lamzin, V. S. (1999). *Nature Struct. Biol.* **6**, 458–463.

Ramakrishnan, C. & Ramachandran, G. N. (1965). *Biophys. J.* **5**, 909–933.

Ren, K., Bannan, J. D., Pancholi, V., Cheung, A. L., Robbins, J. C., Fischetti, V. A. & Zabriskie, J. B. (1994). *J. Exp. Med.* **180**, 1675–1683.

Sundstrom, M., Hallen, D., Svensson, A., Schad, E., Dohlsten, M. & Abrahmsen, L. (1996). *J. Biol. Chem.* **271**, 32212–32216.

Swaminathan, S. & Eswaramoorthy, S. (2000). *Nature Struct. Biol.* **7**, 693–699.

Swaminathan, S., Furey, W., Pletcher, J. & Sax, M. (1995*a*). *Acta Cryst.* D**51**, 1080–1081.

Swaminathan, S., Furey, W., Pletcher, J. & Sax, M. (1995*b*). *Nature Struct. Biol.* **2**, 680–686.

Vallee, B. L. & Auld, D. S. (1990*a*). *Proc. Natl Acad. Sci. USA*, **87**, 220–224.

Vallee, B. L. & Auld, D. S. (1990*b*). *Biochemistry*, **29**, 5647–5659.

Vath, G. M., Earhart, C. A., Monie, D. D., Iandolo, J. J., Schlievert, P. M. & Ohlendorf, D. H. (1999). *Biochemistry*, **38**, 10239–10240.

Vath, G. M., Earhart, C. A., Rago, J. V., Kim, M. H., Bohach, G. A., Schlievert, P. M. & Ohlendorf, D. H. (1997). *Biochemistry*, **36**, 1559–1566.

Weissman, L. (1982). In *Computational Crystallography*, edited by D. Sayre. Oxford: Clarendon Press.

White, J., Herman, A., Pullen, A. M., Kubo, R., Kappler, J. W. and Marrack, P. (1989). *Cell*, **56**, 27–35.